# Lymphocyte recruitment into the aortic wall before and during development of atherosclerosis is partially L-selectin dependent

Elena Galkina,[1,4] Alexandra Kadl,[4] John Sanders,[3,4] Danielle Varughese,[4] Ian J. Sarembock,[3,4] and Klaus Ley[1,2,4]

[1]Department of Biomedical Engineering, [2]Department of Molecular Physiology and Biological Physics, [3]Department of Internal Medicine, and [4]Robert M. Berne Cardiovascular Research Center, University of Virginia, Health Sciences Center, Charlottesville, VA 22908

**Atherosclerosis is an inflammatory disease of large arteries. Flow cytometry of aortic cell suspensions showed that B and T lymphocytes and some macrophages and dendritic cells are already present in the adventitia of normal/noninflamed mouse aortas. Adoptively transferred lymphocytes constitutively homed to the aorta and resided within the adventitia up to 7 d after transfer. Lymphocyte trafficking into normal/noninflamed or atherosclerosis-prone aortas was partially L-selectin dependent. Antigen-activated dendritic cells induced increased T lymphocyte proliferation within the aorta 72 h after adoptive transfer. During progression of atherosclerosis in apolipoprotein-E–deficient mice, the total number of macrophages, T cells, and dendritic cells, but not B cells, increased significantly. This alteration in immune cell composition was accompanied by the formation of tertiary lymphoid tissue in the adventitia of atherosclerotic aortas. These results demonstrate that lymphocytes already reside within the normal/noninflamed aorta before the onset atherosclerosis as a consequence of constitutive trafficking. Atherosclerosis induces the recruitment of macrophages and dendritic cells that support antigen presentation.**

CORRESPONDENCE
Klaus Ley:
klausley@virginia.edu

Abbreviations used: Ab, antibody; *ApoE*$^{-/-}$, apolipoprotein-E–deficient; CMTMR, 5-(and 6)-([{4-chloromethyl}benzoyl] amino) tetramethylrhodamine; HEV, high endothelial venule; oxLDL, oxidized low density lipoprotein; pLN, peripheral LN; *Rag-1*$^{-/-}$ mice, recombination activating gene 1–deficient mice; RBC, red blood cell; vDC, vascular DC; WD, Western Diet.

Atherosclerosis is an inflammatory disease of large and medium-sized arteries that leads to characteristic plaque formation, rupture, and ischemic injury of the dependent vascular bed (1, 2). The possible involvement of the adaptive immune system in atherosclerosis (3) was suggested when T cells and macrophages were detected in human atherosclerotic plaque (4). Further research has implicated immune cells such as T cells (5, 6), B cells (7, 8), monocytes (9, 10), DCs (11, 12), NK cells (13), and NKT cells (14) in the development and progression of atherosclerosis. Although numerous studies were devoted to elucidate the involvement of the immune system in atherosclerosis, no study has provided a complete and quantitative account of the immune cells present in the artery wall. Evidence for the impact of T cells in atherosclerosis comes from studies that identified antigen-specific responses against oxidized low density lipoprotein (oxLDL) and heat shock proteins (15). A Th1 response is prevalent during atherosclerosis and a shift to Th2 promotes antiatherogenic conditions (16). Adoptive transfer of CD4$^+$ lymphocytes increases the progression of atherosclerosis in immunodeficient mice (6).

The presence of B cells in the adventitia of atherosclerotic arteries was described as early as 1981 (17), and CD22$^+$ B cells were found in early fatty streak–type lesions and full-blown atherosclerotic plaques of apolipoprotein-E–deficient (*ApoE*$^{-/-}$) mice (18). Although the impact of B cells on atherosclerosis development was not appreciated for a long time, recent studies show that B cell deficiency increases atherosclerosis in *LDL-receptor*$^{-/-}$ (8) or *ApoE*$^{-/-}$ mice (7). The atheroprotective effect of B cells may be related to natural antibodies (Abs) produced by distinct sets of innate-like B cells, B1 cells, and marginal zone B cells (19).

Vascular DCs (vDCs) are also found in atherosclerotic lesions (11, 12), but it is unclear whether vDCs exist in normal arteries. Autopsy materials from healthy children killed by accidents revealed CD3$^+$ T cells, CD68$^+$ macrophages, and vDCs at bifurcations and curvature sites of normal arteries (20). Dyslipidemia

The online version of this article contains supplemental material.

associated with atherosclerosis alters DC activation and migration in inflamed skin and draining LNs (21). The potential importance of NKT cells for the host response during atherosclerosis was suggested by the finding that CD1d-dependent activation aggravates atherosclerosis (14). Recently, NK cells were also detected in atherosclerotic lesions and a proatherogenic role for NK cells was revealed (13). The most prominent immune cells in atherosclerotic lesions are monocyte-derived macrophages that take up modified LDL and differentiate into foam cells (22, 23). Consistent with the critical role of macrophages in atherosclerosis (for review see reference 24), mice deficient in monocyte CSF are resistant to atherosclerosis development (25).

Limitations inherent in immunohistochemistry-based methods of immune cell detection have so far hampered the quantitative analysis of the inflammatory cell content of the normal and atherosclerotic artery wall. Early attempts were made to analyze the cellular composition in aortas by flow cytometry, but several problems such as high autofluorescence from a large amount of debris and necrotic tissues have been reported (26, 27). The absence of flow cytometry–based methods has also hampered studies on lymphocyte trafficking into the aortic wall under normal and pathological conditions. Here, we use adoptive transfer experiments to demonstrate a role of L-selectin in this process.

Although numerous reports have described the involvement of different leukocyte types in atherosclerosis, few studies investigated the cell composition of the normal aorta (20, 28). Here, we report that T and B cells reside within the adventitia of normal/noninflamed aortas as a consequence of constitutive homing that is partially L-selectin dependent. We used a newly developed flow cytometry–based method to quantitatively investigate the alterations of immune cell composition that occurs during the development and progression of atherosclerosis in $ApoE^{-/-}$ mice, during which tertiary lymphoid tissue is formed in the adventitia of the aortas.

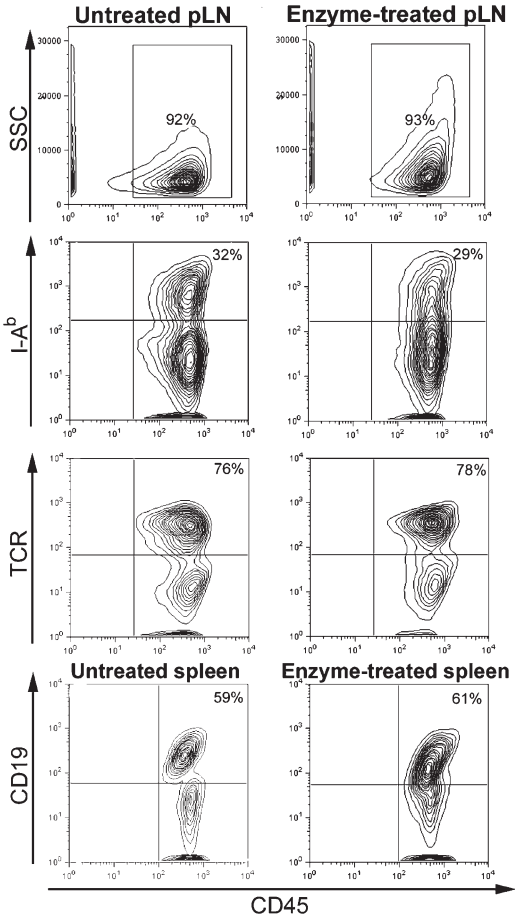


**Figure 1. Method validation for flow cytometry analysis of mouse aorta.** Cell suspensions from pLN or spleen, untreated or treated with enzyme cocktail were stained with anti-CD45 (PE-Texas red), anti-I-$A^b$ (PE), anti-TCRβ (APC), and anti-CD19 (PE-Cy7) Abs; numbers in the gate represent the percentage of $CD45^+$ cells of all analyzed cells. The numbers in the top right quadrant of the bottom six panels represent the percentages of I-$A^{b+}$, $TCR\beta^+$, $CD19^+$ cells among all $CD45^+$ cells.

## RESULTS

### Flow cytometry analysis for the detection of immune cells within the aorta

We used flow cytometry analysis to characterize the immune cell composition within the aortic wall of normal/noninflamed C57BL/6 and atherosclerosis-prone $ApoE^{-/-}$ mice. The average weight of the harvested aortas was 28 ± 2 mg with an average thickness of the adventitia of 146 ± 29 μm and intima + media thickness of 75 ± 6 μm ($n$ = 15). An enzyme cocktail including collagenase I and XI, DNase and hyaluronidase was used to liberate leukocytes from aortic connective tissues. Because enzyme treatment may affect the expression of surface antigens, antigen preservation was confirmed for CD45, I-$A^b$, TCR, CD19 (Fig. 1) and other antigens (Table I) by testing splenocytes or peripheral LN (pLN) cells with and without enzyme treatment.

Possible blood contamination of the carefully rinsed aortic preparations was measured using the presence of red blood cells (RBCs) stained for TER-119, an antigen expressed by RBCs. Based on the number of RBCs and white blood cells in blood ($10 \times 10^6$ cells/μl and $8 \times 10^3$ cells/μl, respectively), <0.02% of blood-derived white blood cells can be expected in the analyzed samples (Fig. S1, available at http://www.jem.org/cgi/content/full/jem.20052205/DC1). To assess the recovery of leukocytes from aortic samples, CD45 expression was determined by quantitative RT-PCR in the material released by enzymatic treatment from aortas of C57BL/6 and $ApoE^{-/-}$ mice, and in the remaining aortic tissue after enzymatic cell release. RT-PCR for blood samples with known leukocyte numbers was performed to obtain a correlation between the number of leukocytes and CD45 mRNA released from the samples. Based on this calibration, we calculated the total number of leukocytes released from the aortas. We found an average of 83% leukocyte release from the aortas of C57BL/6 or $ApoE^{-/-}$ mice (unpublished data).

**Table I.** Antigen markers validated for flow cytometry of aortic leukocytes

| Marker | Ab clone |
|---|---|
| CD45 | 30-F11 |
| CD3ε | 145-2C11 |
| CD5 | 53-7.3 |
| CD8α | 53-6.7 |
| CD19 | 1D3 |
| B220/CD45R | RA3-6B2 |
| CD21 | 7G6 |
| Ig D | 1126c.2a |
| Ig M | R6-60.2 |
| I-$A^b$ | AF6-120.1 |
| Mac-1 | M1/70 |
| Gr-1 | RB6-8C5 |
| 7/4 | 7/4 |
| CD11c | HL3 |
| CD68 | FA-11 |
| F4/80 | BM8 |
| TCRβ | H57-597 |
| CD40 | HM40-3 |
| CD44 | IM7 |
| NK1.1 | PK136 |

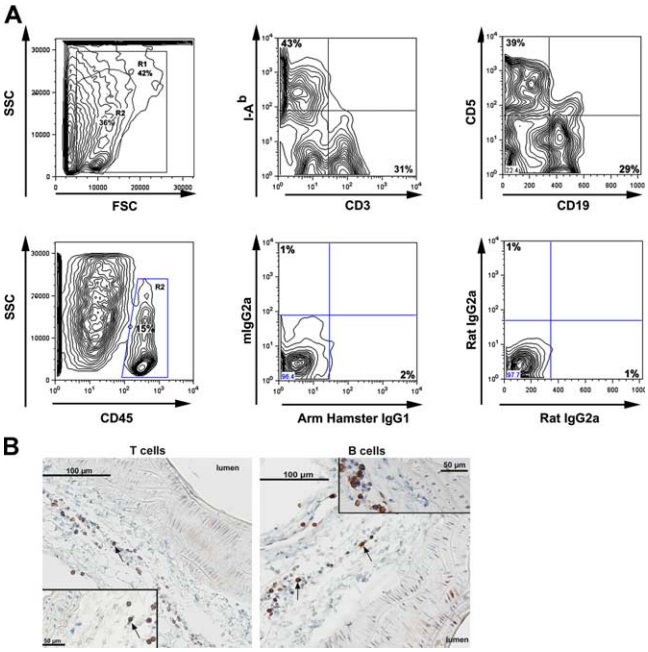


**Figure 2. T and B cells reside within normal/noninflamed aortic wall of C57BL/6 mice.** (A) Leukocytes within the aortic wall of C57BL/6 mice. Aortas from C57BL/6 mice were perfused by cardiac puncture with phosphate-buffered heparin. Collected aortas were digested in enzymes for 1 h at 37°C and cell suspensions were stained with anti-CD45, -CD3, -CD19, -CD5, and I-$A^b$ Abs or with isotype control Abs. To eliminate autofluorescence from debris and necrotic tissues, R1 gate (FSC < 30,000, FSC > 500) was applied for all samples. Then $CD45^+$ cells (gate R2) were defined within R1 gate and further analysis was performed on R1 and R2 cells. (B) B and T cells reside within the aortic wall of C57BL/6 mice. C57BL/6 mice were perfused by cardiac puncture with phosphate-buffered heparin and fixed with 4% paraformaldehyde (PFA). Paraffin-embedded longitudinal sections were stained with anti-CD3 (T cells) or anti-CD20 (B cells) Abs with avidin-biotin technology and counterstained with hematoxylin. Isotype-control Abs showed no staining (not depicted).

### T and B cells reside within the adventitia of normal/noninflamed aortas

To determine whether normal/noninflamed aortas contain any leukocytes within the aortic wall, the aortas from C57BL/6 (Fig. 2 A) and BALB/c (not depicted) mice were digested with enzyme cocktail and analyzed by flow cytometry. The samples of the digested aortas contained endothelial and smooth muscle cells (high FSC, SSC) and some debris (low FSC, SSC) (Fig. 2 A). To identify all leukocytes in the aortas, leukocyte common antigen (CD45) was used and all subsequent analyses were performed on cells gated on CD45. A clearly distinguishable population of $CD45^+$ leukocytes accounts for 3–15% of all aortic cells of C57BL/6 mice (Fig. 2 A). A sizable fraction of aortic leukocytes were T cells as detected by CD3 or CD5 staining. Unexpectedly, we also found abundant B cells as detected by CD19 staining (Fig. 2 A) and B-220 staining (not depicted). Isotype controls verified specific staining. To localize resident lymphocytes, longitudinal aortic sections were stained for B and T cells. Most lymphocytes were found in the adventitia of normal/noninflamed aortas (Fig. 2 B).

### Constitutive L-selectin–dependent homing of T and B cells into the normal/noninflamed aortic wall

Distinct T and B cell populations in normal aortas suggested that constitutive homing mechanisms must exist that allow these cells to traffic into the aortic wall. This process was assessed by adoptive transfer of CFSE-labeled C57BL/6 splenocytes into recombination activating gene 1–deficient (*Rag-1*$^{-/-}$) or C57BL/6 recipient mice. The percentage of fluorescently labeled immigrant leukocytes in C57BL/6 mice represents a minor fraction of endogenous cells in all organs (Fig. S2, available at http://www.jem.org/cgi/content/full/jem.20052205/DC1). To increase the sensitivity of adoptive transfer experiments, we chose to use *Rag-1*$^{-/-}$ recipient mice that have no mature B or T cells (29). Splenic CFSE-labeled B lymphocytes ($CFSE^+/CD19^+$) and T cells ($CFSE^+/CD3^+$) were found within the aortas of recipient mice 24 h after adoptive transfer (Fig. 3 A). Interestingly, T and B lymphocytes migrated about equally to mouse aorta. Although most of the CFSE-labeled cells within the aortic wall were T and B cells, we detected a small fraction of $CFSE^+/CD3^-/CD19^-$ cells within the vessel wall (Fig. 3 A). As expected, T cells homed preferentially to pLN and B cells to spleen (Fig. 3 A).

We further investigated the kinetics of the lymphocyte migration into the normal/noninflamed aortic wall. Both types of lymphocytes constitutively homed into the aortic wall of *Rag-1*$^{-/-}$ recipient mice for at least 24–72 h, reaching

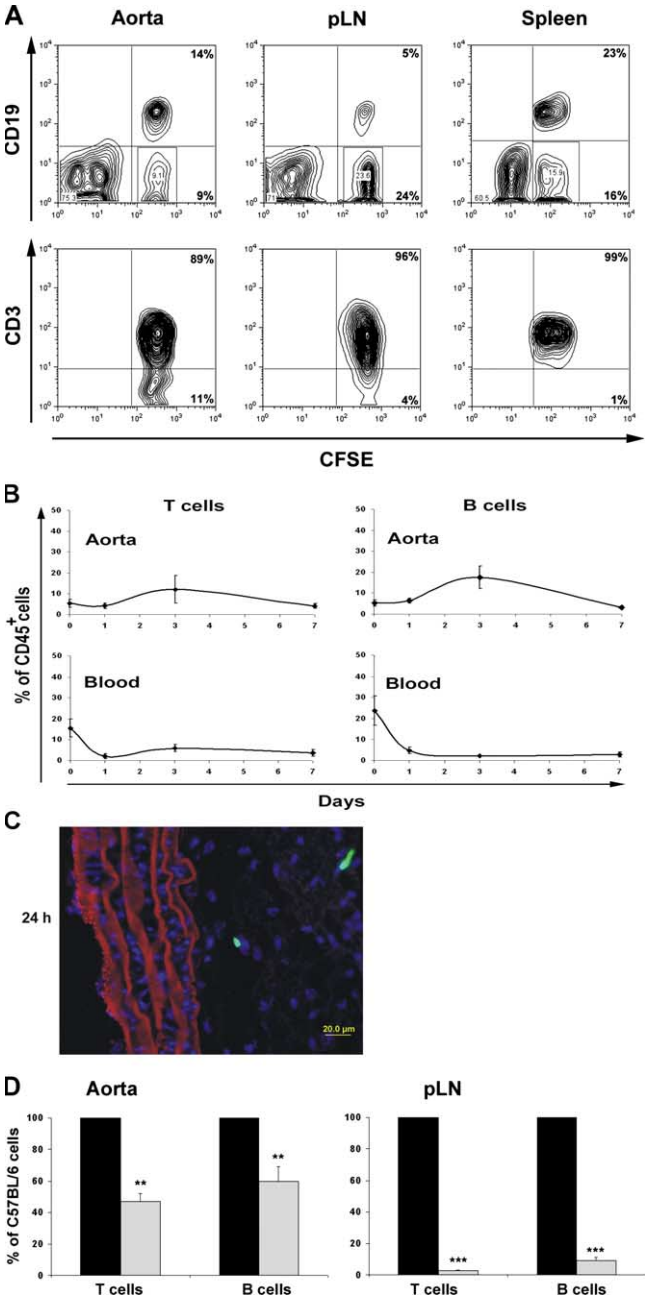


**Figure 3. Constitutive lymphocyte homing into the normal/noninflamed aortic wall.** (A) Adoptive transfer of splenocytes from C57BL/6 mice into *Rag-1*$^{-/-}$ recipient mice. CFSE-labeled splenocytes from C57BL/6 mice were injected i.v. into *Rag-1*$^{-/-}$ mice. After 24 h, cell suspensions from aorta, spleen, and pLN were obtained and stained with Abs against CD3, CD19, and CD45. The top row is gated on CD45$^{+}$; the bottom row is gated on CFSE$^{+}$CD19$^{-}$. Numbers in quadrants are percentage of positive cells. (B) Kinetics of CFSE-labeled lymphocyte migration into *Rag-1*$^{-/-}$ mice ($n$ = 3–9 mice, mean ± SE). *C57BL/6* lymphocytes were labeled with CFSE and 40 × 10$^{6}$ lymphocytes were injected i.v. into *Rag-1*$^{-/-}$ recipient mice. Aorta, blood, spleen, and pLN were collected at 20 min and 1, 3, and 7 d after adoptive transfer; cell suspensions from different organs were stained with anti-CD45, CD19, TCR; and the percentages of CFSE-positive emigrated T and B lymphocytes were determined by flow cytometry. (C) Localization of CFSE-labeled lymphocytes 24 h after adoptive transfer (green-CFSE, blue-DAPI staining). (D) L-selectin–dependent lymphocyte homing into the aorta. C57BL/6 and *L-selectin*$^{-/-}$ splenocytes were labeled with either CFSE or CMTMR, mixed in equal numbers, and injected i.v. into recipient mice. Aortas (left) and LN (right) were collected after 24 h and stained with Abs against CD3, CD19, and CD45$^{+}$. Homing of *L-selectin*$^{-/-}$ lymphocytes (gray bars) is expressed as a percent of C57BL/6 lymphocyte homing (100%, black bars). Results show mean ± SE from at least four recipients from at least three independent experiments. **, $P < 0.01$; ***, $P < 0.001$.

a maximum at 72 h after transfer (Fig. 3 B). Only a few T and B cells remained in the blood (Fig. 3 B). This homing pattern was confirmed in C57BL/6 mice (unpublished data). To determine whether CFSE-labeled lymphocytes migrated from the lumen of large aortic vessel or homed from vasa vasorum that penetrate adventitial tissues, we analyzed the distribution of CFSE-labeled lymphocytes 25 min and 24 h after adoptive transfer. CFSE-labeled lymphocytes were detected mostly if not exclusively within the adventitia, but not within the intima or media layers of the aortas 25 min (not depicted) and 24 h (Fig. 3 C) after adoptive transfer.

To explore the molecular mechanisms of lymphocyte homing to the aortic wall, we performed competitive homing assays using CFSE-labeled splenocytes from L-selectin knockout (*L-selectin*$^{-/-}$) mice (30) and 5-(and 6)-([{4-chloromethyl}benzoyl]amino) tetramethylrhodamine (CMTMR)-labeled splenocytes from C57BL/6 mice. *L-selectin*$^{-/-}$ T or B lymphocyte migration into the aortic wall was only 50% of that of wild-type lymphocytes (Fig. 3 D). Similar results were obtained at 72 h after adoptive transfer (unpublished data). Although L-selectin absence significantly reduced lymphocyte migration into the aortas, it did not change the localization within the aortic wall (unpublished data). These results provide the first evidence that L-selectin is involved in the constitutive homing of lymphocytes into the noninflamed aortic wall. Homing to pLN, which is known to be L-selectin dependent (Fig. 3 D), and spleen (reference 30 and unpublished data) showed the expected patterns.

### Alterations of the immune cell composition accompany the development and progression of atherosclerosis

The process of atherosclerotic plaque formation is characterized by the influx of monocytes/macrophages and T cells into neointimal lesion sites, but the number and nature of inflammatory cells that accumulate within the aortic wall have not been determined. Therefore, we analyzed the cellularity of aortas under normal conditions (C57BL/6 mice), mild atherosclerosis (*ApoE*$^{-/-}$ mice), and advanced atherosclerosis (*ApoE*$^{-/-}$ mice fed Western Diet [WD]). Normal/noninflamed aortas contain 0.6 ± 0.10$^{6}$ leukocytes per aorta (Fig. 4 A). A doubling to 1.2 ± 0.10$^{6}$ leukocytes was detected in the aortas of *ApoE*$^{-/-}$ fed chow diet, with a further increase to 2.6 ± 0.5 × 10$^{6}$ cells in *ApoE*$^{-/-}$ mice fed WD (Fig. 4 A).

During atherosclerosis development, the percentage of T cells (Fig. 4 B) within the aortas did not increase significantly (30.4 ± 2.8% and 31.6 ± 3.1%, $n$ = 21 and $n$ = 26 for

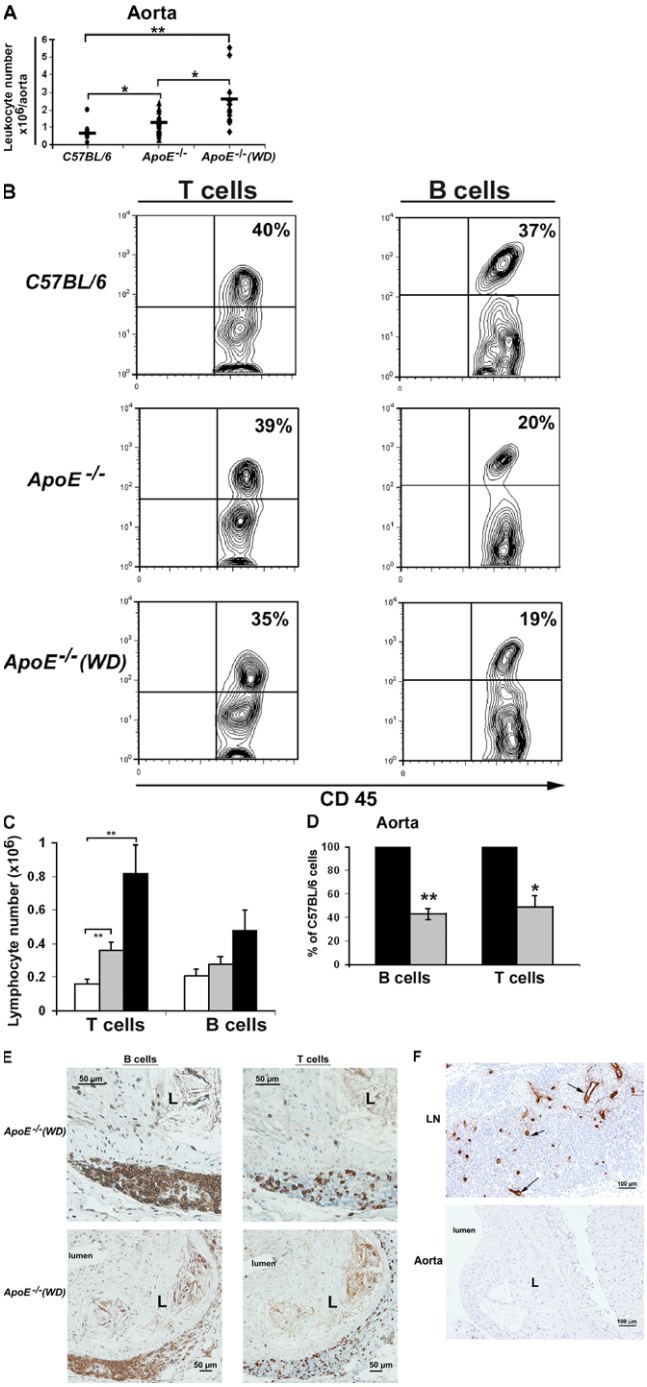


**Figure 4. T and B lymphocyte compartment alterations during atherosclerosis.** (A) Total leukocyte number in the aorta of 33–35 wk old C57BL/6, *ApoE*$^{-/-}$ and *ApoE*$^{-/-}$ *(WD* for 20 wk) mice. Cells were liberated from the aortic tissues and the total leukocyte number was determined ($n$ = 14–23 mice). Mean is indicated by horizontal bar. *, $P < 0.05$; **, $P < 0.01$. (B) T and B lymphocyte compartments in C57BL/6, *ApoE*$^{-/-}$ and *ApoE*$^{-/-}$ *(WD)* mice. Cell suspensions from aortas of C57BL/6 ($n$ = 12, white bar), *ApoE*$^{-/-}$ ($n$ = 26, gray bar) and *ApoE*$^{-/-}$ *(WD)* ($n$ = 21, black bar) mice were stained with Abs against CD45, TCRβ (left), and CD19 (right). The number in the quadrants represents the percentage of positive cells. All plots were gated on CD45$^+$ cells. (C) Total T and B lymphocyte numbers in the aorta of C57BL/6, *ApoE*$^{-/-}$ and *ApoE*$^{-/-}$ *(WD)* mice were calculated from the total cell number and the percentage of each population. Results are means ± SE ($n$ = 12–26). **, $P < 0.01$. (D) L-selectin–dependent lymphocyte homing into the atherosclerotic aorta. C57BL/6 and *L-selectin*$^{-/-}$ splenocytes were labeled with either CFSE or CMTMR, mixed in equal number, and injected i.v. into *ApoE*$^{-/-}$ (WD) recipient mice. Aortas were collected after 24 h and stained with Abs against CD3, CD19, and CD45. Homing of *L-selectin*$^{-/-}$ lymphocytes (gray bars) is expressed as the percentage of C57BL/6 lymphocyte homing (100%, black bars). Results show mean ± SE from at least four recipients from at least three independent experiments. **, $P < 0.01$. (E) B (left) and T (right) cells form organized lymphoid tissue in the adventitia of *ApoE*$^{-/-}$ *(WD)* mice. Paraffin-embedded sections (5 μm) were stained with Abs against CD20 and CD3, respectively, and counterstained with hematoxylin. Isotype-control Abs showed no staining (not depicted). L, neointimal lesion. (F) MECA-79 is expressed in LN (top), but not in lymphoid tissue in the aortas of *ApoE*$^{-/-}$ *(WD)* mice. Isotype-control Abs showed no staining (not depicted).

*ApoE*$^{-/-}$ and *ApoE*$^{-/-}$ [WD], respectively) compared with C57BL/6 mice (26.1 ± 2.5%, $n$ = 12). However, as the result of the increased total cell number, absolute T cell content doubled in aortas of *ApoE*$^{-/-}$ mice and quintupled in *ApoE*$^{-/-}$ (WD) mice compared with the number of T cells from the aortic wall of C57BL/6 mice (Fig. 4 C). B cells accounted for 32.6 ± 3.3% ($n$ = 12) in aortas of C57BL/6 mice. The percentage of B cells significantly decreased in the aortas of *ApoE*$^{-/-}$ and *ApoE*$^{-/-}$ (WD) mice (23.4 ± 2.7% and 18.5 ± 2.9%, $n$ = 21 and $n$ = 26, respectively; $P < 0.05$; Fig. 4 B). The absolute number of B cells in aortas of *ApoE*$^{-/-}$ mice remained similar to control mice (Fig. 4 C).

To determine the possible role of L-selectin in lymphocyte homing into atherosclerotic aortas, equal numbers of splenic C57BL/6 and *L-selectin*$^{-/-}$ lymphocytes were adoptively transferred into *ApoE*$^{-/-}$ *(WD)* mice for 24 h. As shown in Fig. 4 D, B cells from *L-selectin*$^{-/-}$ mice displayed a 57% reduction in migration into atherosclerotic aortas of recipient mice in comparison with migration of C57BL/6 B lymphocytes. *L-selectin*$^{-/-}$ T cells demonstrated a similar 50% reduction in homing to atherosclerotic aortas (Fig. 4 D). The partial reduction of lymphocyte homing in the absence of L-selectin suggests that migration of T and B lymphocytes into the atherosclerotic aorta is regulated by L-selectin and other adhesion molecules.

To analyze the spatial distribution of T and B cells, longitudinal aortic sections from atherosclerotic *ApoE*$^{-/-}$ *(WD)* mice were stained for CD3 and CD19 (Fig. 4 E). Both B and T cells were found under the medial layer within the adventitia of aortas in ordered structures close to atherosclerotic lesions (Fig. 4 E), but no big lymphocyte conglomerates were found in the adventitia of areas of the aorta that did not contain plaques (not depicted). As expected, some lymphocytes were detected within atherosclerotic plaque (unpublished data). Interestingly, MECA-79 Ab that recognizes a major class of L-selectin ligands in high endothelial venules (HEVs) and activated endothelium (31) showed no staining within the lymphoid aggregates residing under the media layer (Fig. 4 F, bottom). Like other LNs, para-aortic LNs have MECA-79$^+$

HEVs, but we never detected MECA-79 staining in any of the analyzed aortas, confirming that our vessels were harvested without contamination from para-aortic LNs. As a positive control, MECA-79 staining is shown in inguinal LN (Fig. 4 F, top).

The involvement of macrophages in atherosclerosis is well documented and an accumulation of monocyte-derived macrophages within early and advanced atherosclerotic lesions has been shown by immunohistochemistry (for review see reference 24). Resident macrophages (Mac-$1^+$/I-$A^{b+}$/$CD45^+$) accounted for 6.2 ± 1.7% of all leukocytes in the aortas of *C57BL/6* mice ($n = 10$), but this fraction increased to 16.5 ± 2.5% and 25.1 ± 4.5% in *ApoE*$^{-/-}$ mice on chow ($n = 18$) and WD ($n = 16$), respectively (Fig. 5 A, left). The total number of macrophages increased 6- and 20-fold in *ApoE*$^{-/-}$ and *ApoE*$^{-/-}$ *(WD)*, respectively (Fig. 5 B). These macrophages also expressed CD68 (Fig. S3, available at http://www.jem.org/cgi/content/full/jem.20052205/DC1) and elevated levels of I-$A^b$, indicating an activated phenotype. To further characterize the distribution of macrophages within normal/noninflamed and atherosclerotic aortas, longitudinal sections of C57BL/6 and *ApoE*$^{-/-}$ *(WD)* aortas were stained with mAb Mac-2. Some macrophages were detected within the adventitia of normal C57BL/6 aortas and increased macrophage staining was detected within the lesions and adventitia of *ApoE*$^{-/-}$ *(WD)* mice (Fig. S4, available at http://www.jem.org/cgi/content/full/jem.20052205/DC1). DCs ($CD11c^+$/I-$A^{b+}$) were present in normal mouse aortas, consistent with a previous report in human vessels (12), and DCs were also detected in the vessel wall of *ApoE*$^{-/-}$ and *ApoE*$^{-/-}$ *(WD)* mice (Fig. 5 A, right). Although the percentage of DCs within the atherosclerosis-prone aortas did not change dramatically, the absolute DC number was elevated threefold within the aortas of *ApoE*$^{-/-}$ *(WD)* mice compared with C57BL/6 mice (Fig. 5 B).

To graphically depict total aortic wall content and proportions of inflammatory cells, we constructed pie charts (Fig. 5 C). T and B cells are the major leukocyte populations in the aortas C57BL/6 mice, with a small subset of macrophages and DCs. Other leukocytes including neutrophils, NK cells, and NKT cells account for 20–30% of all leukocytes. In *ApoE*$^{-/-}$ mice, the total leukocyte number increases, with an expanded macrophage and a reduced B cell fraction. Feeding *ApoE*$^{-/-}$ mice a WD further expands the macrophage population and slightly augments T cells. Interestingly, the fraction of B cells, but not their absolute number, shrinks with the progression of atherosclerosis.

### Immunization with antigen-activated DCs leads to proliferation of adventitial T lymphocytes within the aorta

Activated lymphocytes have been detected within atherosclerosis-prone aortas and the progression of atherosclerosis is characterized by a Th1 response, but little is known about the kinetics of the T cell activation within the aorta during atherosclerosis. Hypercholesterolemia is associated with T cell responses to plaque antigens like heat shock protein-60 and

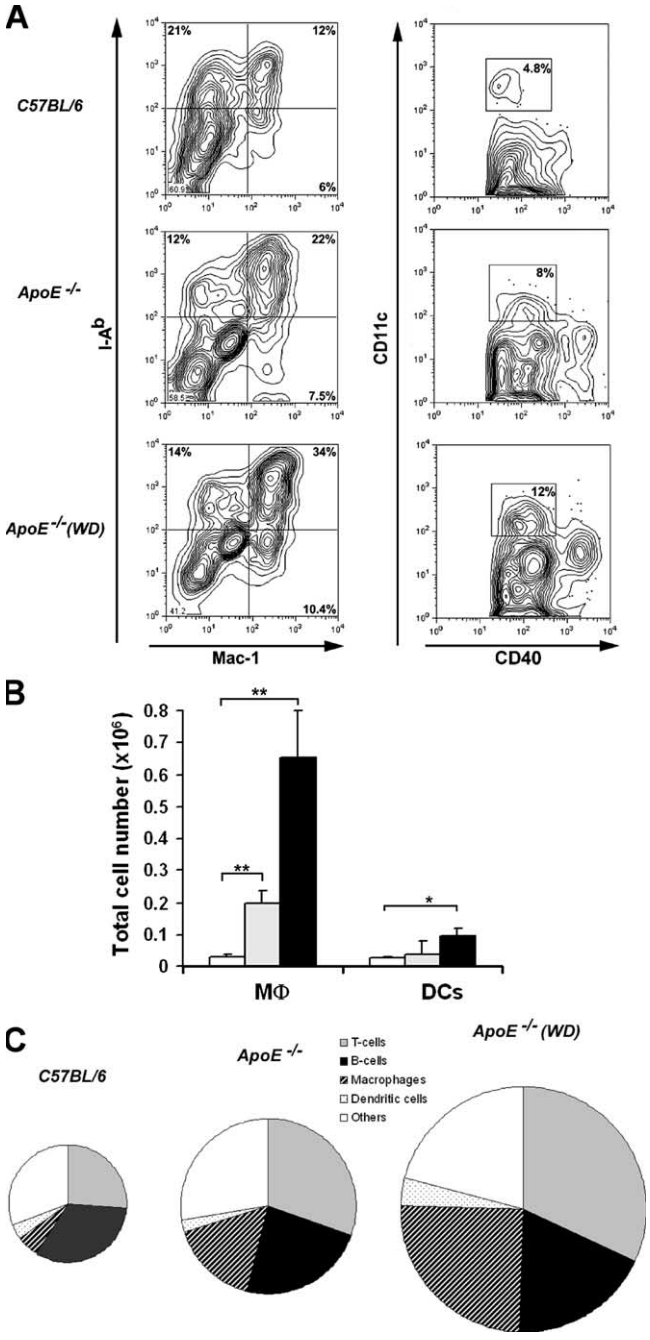


**Figure 5. Immune cell composition during the development and progression of atherosclerosis.** (A) Macrophages and dendritic cells in C57BL/6, *ApoE*$^{-/-}$ and *ApoE*$^{-/-}$ *(WD)* mice. Cell suspensions from mouse aortas were stained with Abs against CD45, I-$A^b$, Mac-1 (left) and CD11c and CD40 (right). Plots gated on $CD45^+$ cells (macrophages) and on $CD45^+$/$CD40^+$ (DCs). Representative plots from one experiment are shown. (B) Total number of macrophages and dendritic cells in the aortas of C57BL/6 (white bars), *ApoE*$^{-/-}$ (gray bars), and *ApoE*$^{-/-}$ *(WD)* (black bars) mice, calculated based on the percentage of each population and the total number of leukocytes from the aortas. Results mean ± SE ($n = 7$–17). *, $P < 0.05$; **, $P < 0.01$. (C) Alterations in the immune cell composition during development and progression of atherosclerosis. The area of each circle is proportional to the number of $CD45^+$ cells.

oxLDL (16); however, the role of these antigens in the initiation and maintenance of atherosclerosis is unclear. To detect an antigen-specific T cell response in the aorta and to increase the frequency of antigen-specific T lymphocytes during the first days of activation, we used OT-1 transgenic mice that express a transgenic MHC class I–restricted TCR (OT-1) on the *RAG-2*$^{-/-}$ background (32). Adoptively transferred bone marrow–derived DCs activated with OVA peptide induced profound proliferation of TCR-specific lymphocytes in spleen and aortas of OT-1 recipient mice that is reflected by an elevated percentage of BrdU$^+$ CD8$^+$ T cells (Fig. 6, A and B) and elevated levels of CD44 on T cells (Fig. 6 A). As a positive control, we detected elevated proliferation of T lymphocytes in pLN (unpublished data) and spleen, but not in blood of recipient mice (Fig. 6 B).

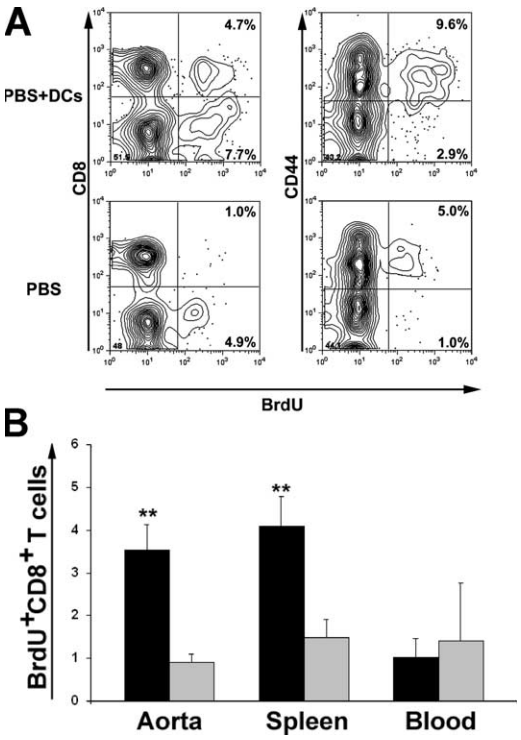


**Figure 6. Immunization with antigen-activated DCs leads to proliferation of adventitial T lymphocytes within the aorta.** CD40L-activated DCs were pulsed with antigen peptide and either $10^5$ bone marrow–derived DCs in 200 μl PBS or 200 μl PBS were injected i.v. into OT-1 transgenic recipient mice. At 48 and 60 h, 1 mg BrdU was injected i.p. Aorta, pLN, spleen, and blood were collected 72 h after transfer, and the cell suspensions were stained with anti-CD45, -CD8, -CD44, and anti-BrdU Abs. All plots were gated on CD45$^+$ lymphocyte gate. (A) Representative plots from one experiment. The numbers in quadrants represents BrdU$^+$ cells. (B) The percentage of BrdU$^+$ CD8$^+$ T cells in the aortas and spleens of OT-1 control (gray bars) or immunized OT-1 recipient mice (black bars) are presented. Results mean ± SE ($n = 8$). **, $P < 0.01$.

## DISCUSSION

Our studies show that T and B lymphocytes reside within the adventitia of the normal/noninflamed aortic wall as the result of constitutive, partially L-selectin–dependent lymphocyte trafficking into the vessel wall. Aortic T and B cells together with resident macrophages and DCs comprise a large population of immune cells in the aorta, equal to numbers found in a small lymph node. During development and progression of atherosclerosis, these populations form adventitial lymphoid structures with reduced B cell and increased macrophage and T cell contents.

The involvement of the adaptive immune system in atherosclerosis has been well documented in several reports (33–35). However, the quantitative detection of different types of immune cells within the aortic wall was limited by the existing methods for study of atherosclerosis. Here, we describe a flow cytometry–based method to analyze the immune cell composition in the normal/noninflamed and atherosclerotic aortas. A clear and surprising result is that the normal/noninflamed aorta of C57BL/6 mice contains a distinguishable population of CD45$^+$ leukocytes. T and B cells were major fractions of this population. Immunohistochemistry of C57BL/6 aortas confirmed the flow cytometry results and, in addition, revealed that both lymphocyte types reside within the aortic adventitia. This may be one of the reasons why the existence of lymphocyte populations in the aorta was not broadly appreciated in histological studies because the major focus of these previous investigations was on the aortic intimal and medial layers (4, 18).

Our study shows that naive T and B cells constitutively migrate into the normal/noninflamed aorta and reside within the vessel wall after adoptive transfer. Leukocyte trafficking within postcapillary venules requires selectin-dependent rolling, integrin-dependent firm adhesion, and subsequent diapedesis (36). The adhesion cascade that occurs within large vessels involves P-selectin (37) and growth-related oncogene (Gro) chemokines (38). L-selectin/PSGL-1–dependent leukocyte–leukocyte interactions have been described in mouse aortas (39), but their role in immune cell recruitment was not studied. Here, we show that both B and T cells enter the noninflamed aortic wall through a partially L-selectin–dependent process. Our short-term trafficking study suggests that lymphocytes may constitutively enter the adventitia through vasa vasorum.

Atherosclerotic plaques are thought to consist of lipid-laden monocytes, macrophages, and T cells (2). Here, we present the first actual leukocyte numbers in the normal/noninflamed vessel, and describe the dynamics of the influx of CD45$^+$ cells into the aortas of *ApoE*$^{-/-}$ and *ApoE*$^{-/-}$ *(WD)* mice. We found a significant increase in the percentage and total number of T cells and macrophages within the atherosclerotic wall. These results confirm and extend earlier observations suggesting a crucial role of monocytes/macrophages (1, 10, 22) and T cells (5, 6, 15) in the initiation and maintenance of atherosclerosis. The existence of T cells in the atherosclerotic plaques was reported in the early 1990's (4, 40); however, the quantitative T cell proportion at the different stages of atherosclerosis has not been investigated. Our data provide evidence that T cells are a major subset of

$CD45^+$ cells not only within the normal aortas, but also in the inflamed aortas of *ApoE*$^{-/-}$ mice. B lymphocytes were not known to reside in the normal vessel wall, but actually account for 33% of all aortic leukocytes in *C57BL/6* mice. Interestingly, the total B cell number does not change much during the progression of atherosclerosis; however, the percentage of B cells among $CD45^+$ cells is significantly reduced in *ApoE*$^{-/-}$ mice compared with C57BL/6. The decrease of the B cell percentage in atherosclerotic aortas in parallel with the atherosclerosis progression suggests that B cells may play a protective role locally within the aortic wall. Innate-like B cells, B1 cells, and marginal zone B cells represent a major source of natural Abs (41). Some of these natural Abs recognize the phosphorylcholine moiety present in oxLDL and inhibit scavenger receptor-mediated binding of oxLDL by macrophages (42). Some resident aortic B cells may produce natural Abs and minimize the presence of "free oxLDL" within the aortic wall.

Interestingly, the entry of T and B lymphocytes into atherosclerosis-prone aortas was also partially L-selectin dependent. Although we found no MECA-79 expression within the aortic wall, it is possible that other L-selectin ligands may be expressed within the aorta, or L-selectin might mediate secondary capture (39) that allows lymphocyte migration into the vessel wall.

Electron microscopy of normal/noninflamed aortas reveals a small number of vDCs displaying distinct unique ultrastructural features (43). In this study, vDCs were found in aortic wall of *C57BL/6* as well as *ApoE*$^{-/-}$ mice by flow cytometry. We detect no changes in the vDC percentage within the aortas during the development of atherosclerosis; however, a significant increase in total vDCs number is observed in atherosclerotic aortas of *ApoE*$^{-/-}$ *(WD)* mice. This finding is supported by data that during progressive atherosclerosis DCs show impaired exit from aortas, leading to DC accumulation within the vessel wall (44).

The existence of vascular-associated lymphoid tissue was first proposed by Wick et al. (20) and, here, we confirm and extend this finding. The fact that T cells, B cells, and vDCs are permanent residents even in the normal/noninflamed aortas suggests that the immune system may be involved in homeostatic regulation of immune responses within the vessel wall. In atherosclerotic vessels, lymphocytes reside in ordered structures exclusively within the adventitia at sites of atherosclerotic lesions. It is well known that in the adult immune system, a state of activation is necessary to induce the formation of lymphoid tissue (45). We propose that during the development of atherosclerosis, pathological immune activation occurs and leads to the formation of adventitial lymphoid-like tissues with subsequent local inflammation. Similar structures have been recently reported in aged *ApoE*$^{-/-}$ mice on chow diet (46). Interestingly, we found no HEVs expressing MECA-79 antigen, suggesting that homing mechanisms to vascular-associated lymphoid tissue are different from LNs.

Several papers have reported that T cells and particularly Th1 type lymphocytes play a proatherogenic role (1). In the present study, we show that antigen-pulsed DCs induced increased proliferation of antigen-specific $CD8^+$ T lymphocytes in the aortas of recipient mice at 72 h after adoptive transfer. These results provide the first evidence that T cells residing within the aorta can be activated by antigen-presenting cells, suggesting that this process may be important in the initiation and/or progression of atherosclerosis.

Our studies establish a firm basis for an involvement of the local vascular immune system in the development and progression of atherosclerosis. The existence of robust leukocyte populations in the adventitia of normal aortas provides evidence for a well-developed vascular lymphoid tissue in large arteries and an important role of the adventitia as a site of localization of immune cells under normal and atherosclerotic conditions. Interactions between antigen-presenting cells and T cells may determine the development and progression of atherosclerotic disease.

## MATERIALS AND METHODS

**Animals.** L-selectin$^{-/-}$ (30), ApoE$^{-/-}$ (47), and Rag-1$^{-/-}$ (29) mice (The Jackson Laboratory) were maintained on the C57BL/6 background, OT-1 mice (32) (provided by V. Engelhard, University of Virginia, Charlottesville, VA) were maintained on Rag-2$^{-/-}$ background under specific pathogen-free conditions at the University of Virginia. Beginning at 14–15 wk of age, female and male ApoE$^{-/-}$ mice were fed WD. After 19–20 wk of WD, ApoE$^{-/-}$ on WD and age-matched ApoE$^{-/-}$ on chow diet and C57BL/6 mice were used. All animal experiments were approved by the University of Virginia Animal Care and Use Committee, in accordance with Association for Assessment and Accreditation of Laboratory Animal Care guidelines.

**Flow cytometry analysis of immune cells within mouse aorta.** C57BL/6, *ApoE*$^{-/-}$ *or ApoE*$^{-/-}$ *(WD)* mice were anesthetized and their vasculature was perfused by cardiac puncture with PBS containing 20 U/ml of heparin to remove blood from all vessels. Under a dissection microscope, we carefully harvested whole aortas by pulling off all of the adipose tissue and collecting all aortic layers including the adventitia. To fully characterize the collected aortas, we measured aortic wall thickness and adventitial thickness in paraffin-cut sections. In addition, the dissected aortas were weighed to control the total amount of collected aortic tissues. Harvested aortas were microdissected and digested with 125 U/ml collagenase type XI, 60 U/ml hyaluronidase type I-s, 60 U/ml DNase1, and 450 U/ml collagenase type I (all enzymes were obtained from Sigma-Aldrich) in PBS containing 20 mM Hepes at 37°C for 1 h. A cell suspension was obtained by mashing the aorta through a 70-μm strainer. Cells were incubated with Abs for 20 min at 4°C, washed twice, and incubated with secondary Abs for an additional 20 min. After washing, immunofluorescence was detected by flow cytometry (FACSCalibur or CyanADP), data were analyzed using WinMDI (The Scripps Research Institute) or FlowJO (Tree Star Inc.) software. Abs used were as follows: allophycocyanin (APC)-Cy7 or PE-Texas red-CD45, FITC, PE or PerCP-CD3, FITC, APC-TCRβ, PE-Cy5 or APC-CD19, PE-B220, PE-I-$A^b$, PerCP-Cy5.5-Mac-1, PE or APC-CD11c (all Abs were obtained from BD Biosciences) and FITC-CD68 (Serotec). In some experiments, the aortas from two to three mice were pooled and analyzed. In some experiments, LN or spleens from C57BL/6 mice were collected and split in two parts: one part of pLN (or spleen) was treated with the enzyme cocktail (see previous paragraph) and the other was kept at 4°C. After 1 h, the expression of CD45, TCR, CD19, I-$A^b$ antigens was determined by flow cytometry.

**In vivo trafficking experiments.** Splenic cells from C57BL/6 mice were labeled with 0.1 μM CFSE (Invitrogen) in PBS at 37°C for 20 min and washed twice in PBS containing 1% FCS. $40 \times 10^6$ of labeled cells in 0.2 ml of PBS were injected into tail veins (i.v.) of C57BL/6 or *Rag-1*$^{-/-}$ recipient

mice. Cell suspensions were obtained from aortas, spleen, pLN, and blood and stained with anti-CD3 (PE), anti-CD19 (APC), and anti-CD45 (PerCP) Abs. The percentages of CFSE-labeled T and B cells in the total population of $CD45^+$ cells were determined by flow cytometry. Competitive homing assays were conducted by staining *L-selectin*$^{-/-}$ and C57BL/6 splenocytes with either 0.1 μM CFSE in PBS or 7 μM CMTMR (Invitrogen) in RPMI 1640 at 37°C for 20 min. In some experiments, dyes were switched. Labeled cells were mixed at a 1:1 ratio in the starting population, and $35 \times 10^6$ labeled cells of each population were injected i.v. into recipient mice. At 24 and 72 h, aortas, spleen, blood, and pLN were harvested. Aortas were digested as described in flow cytometry analysis and cell suspensions from aortas, spleen, and blood were stained with anti-CD3, anti-CD19 and with Ab against CD45. CFSE and CMTMR-labeled cells as a fraction of gated $CD45^+$ lymphocytes in the aortic wall, pLN, spleen, and blood were determined by flow cytometry. Wild-type lymphocytes were set at 100%, and homing of *L-selectin*$^{-/-}$ lymphocytes was expressed relative to wild-type cells. If the ratio of T or B cells (the percentages of T and B cells were determined by flow cytometry) in the injected population deviated from 1, a correction coefficient was applied to normalize the percentage of immigrated T and B cells.

**Immunohistochemistry.** Mice were perfused by cardiac puncture with 40 ml PBS containing 20 U/ml of heparin and fixed with 4% PFA. Serial aortic longitudinal and inguinal LN paraffin-embedded sections were cut (5 μm). Tissues were stained with anti-CD3, anti-CD20 (both obtained from Santa Cruz Biotechnology, Inc), MECA-79 (BD Biosciences), or isotype control Abs with avidin-biotin technology. Frozen sections were stained with biotin anti–Mac-2 Ab (Cedarlane, Lab. Limited) after streptavidin- Alexa 488 (Invitrogen) staining. To analyze the location of CFSE-labeled lymphocytes in the aortas of recipients, CFSE-labeled *C57BL/6* splenic cells were injected (see previous paragraph) and the aortas were collected 25 min and 24 h after adoptive transfer. Serial longitudinal frozen section were cut and stained with DAPI. Images were acquired using the 10, 20, or 40× objective on a microscope (Olympus) equipped with a digital camera (Olympus) using the ImagePro Plus software program in the Academic Computing Health Sciences Center at the University of Virginia.

**Real-time RT-PCR.** Aortas from C57BL/6 or *ApoE*$^{-/-}$ mice were isolated and treated with the enzymes as described for flow cytometry analysis. RNA was isolated using TRIzol (Invitrogen) either from aortic cell suspension or from the remaining aortic material after enzymatic cell release. Equal volumes were reverse transcribed and analyzed for CD45 and $\beta_2$-microglobulin expression using specific primers (CD45-forward, 5′-CCTCCAAGCACAACCATAGC-3′ and CD45-reverse, 5′-CAATCCTCATTTCCACACTTAGC-3′ for CD45; and $\beta_2$-microglobulin-forward, 5′-ATTCACCCCCACTGAGACTG-3′ and $\beta_2$-microglobulin-reverse, 5′-TGCTATTTCTTTCTGCGTGC-3′). These primers were designed to span an intron to avoid coamplification of genomic DNA. RT-PCR was performed using the iCycler MyiQ Real-Time PCR detection system using Sybr green I. The specificity of the amplification was controlled by electrophoresis of the PCR product. The ratio between CD45 and $\beta_2$-microglobulin expression was calculated. To quantitate absolute numbers of leukocytes in the tissue, a standard curve for CD45 expression was prepared from serial dilutions of blood leukocytes ($3.2 \times 10^3$–$10^7$ leukocytes).

**Immunizations.** DCs were generated by culturing mouse bone marrow cells in GM-CSF and IL-4 (BD Biosciences), as described previously (48). CD40L-activated DCs were pulsed with 10 μg/ml $\beta_2$-microglobulin and 10 μg/ml of OVA-peptide (SIINFEKL) and incubated at 37°C for 1 h. $10^5$ pulsed DCs in 200 μl PBS or 200 μl PBS (control) were injected i.v. into OT-1 transgenic mice. Recipient mice received 1 mg BrdU in 200 μl PBS i.p. at 48 and 60 h after DC transfer; aorta, spleen, pLN, and blood were collected 12 h later. Incorporation of BrdU into DNA was measured by flow cytometry using anti-BrdU–FITC (BD Biosciences) as per the manufacturer's protocol.

**Statistical analysis.** Data are represented as the mean ± SE. Differences in lymphocyte homing in the adoptive transfer experiments were compared using paired Student's *t* test. Other comparisons were made using unpaired Student's *t* test.

**Online supplemental material.** Fig. S1 shows that rinsing and vessel dissection results in minimal blood contamination. Fig. S2 demonstrates constitutive lymphocyte trafficking into the aortic wall of C57BL/6 recipient mice. Fig. S3 shows $CD68^+$/I-$A^{b+}$ macrophages during the development and progression of atherosclerosis. Fig. S4 illustrates the localization of macrophages within the normal/noninflamed and atherosclerotic aortas. Online supplemental material is available at http://www.jem.org/cgi/content/full/jem.20052205/DC1.

We thank M. Solga and J. Lanningan who helped us with 7-color flow cytometry; B. Harry for the technical help; S. Sheasley-O'Neill, C.C. Brinkman, and V.H. Engelhard for the advice in OT-1 experiments; and G.K. Hansson for critical reading.

This work was supported by National Institutes of Health grant nos. HL58108 and POI HL55798 (to K. Ley) and AHA 0525532U (to E. Galkina).

The authors declare that they have no competing financial interests.

**Submitted: 1 November 2005**
**Accepted: 28 March 2006**

## REFERENCES

1. Libby, P. 2002. Inflammation in atherosclerosis. *Nature*. 420:868–874.
2. Ross, R. 1999. Atherosclerosis–an inflammatory disease. *N. Engl. J. Med*. 340:115–126.
3. Hansson, G.K. 2005. Inflammation, atherosclerosis, and coronary artery disease. *N. Engl. J. Med*. 352:1685–1695.
4. Jonasson, L., J. Holm, O. Skalli, G. Bondjers, and G.K. Hansson. 1986. Regional accumulations of T cells, macrophages, and smooth muscle cells in the human atherosclerotic plaque. *Arteriosclerosis*. 6:131–138.
5. Buono, C., H. Pang, Y. Uchida, P. Libby, A.H. Sharpe, and A.H. Lichtman. 2004. B7-1/B7-2 costimulation regulates plaque antigen-specific T-cell responses and atherogenesis in low-density lipoprotein receptor-deficient mice. *Circulation*. 109:2009–2015.
6. Zhou, X., A. Nicoletti, R. Elhage, and G.K. Hansson. 2000. Transfer of CD4(+) T cells aggravates atherosclerosis in immunodeficient apolipoprotein E knockout mice. *Circulation*. 102:2919–2922.
7. Caligiuri, G., A. Nicoletti, B. Poirier, and G.K. Hansson. 2002. Protective immunity against atherosclerosis carried by B cells of hypercholesterolemic mice. *J. Clin. Invest*. 109:745–753.
8. Major, A.S., S. Fazio, and M.F. Linton. 2002. B-lymphocyte deficiency increases atherosclerosis in LDL receptor-null mice. *Arterioscler. Thromb. Vasc. Biol*. 22:1892–1898.
9. Aqel, N.M., R.Y. Ball, H. Waldmann, and M.J. Mitchinson. 1984. Monocytic origin of foam cells in human atherosclerotic plaques. *Atherosclerosis*. 53:265–271.
10. Glass, C.K., and J.L. Witztum. 2001. Atherosclerosis. The road ahead. *Cell*. 104:503–516.
11. Bobryshev, Y.V., and R.S. Lord. 1998. Detection of vascular dendritic cells accumulating calcified deposits in their cytoplasm. *Tissue Cell*. 30: 383–388.
12. Yilmaz, A., M. Lochno, F. Traeg, I. Cicha, C. Reiss, C. Stumpf, D. Raaz, T. Anger, K. Amann, T. Probst, et al. 2004. Emergence of dendritic cells in rupture-prone regions of vulnerable carotid plaques. *Atherosclerosis*. 176:101–110.
13. Whitman, S.C., D.L. Rateri, S.J. Szilvassy, W. Yokoyama, and A. Daugherty. 2004. Depletion of natural killer cell function decreases atherosclerosis in low-density lipoprotein receptor null mice. *Arterioscler. Thromb. Vasc. Biol*. 24:1049–1054.
14. Tupin, E., A. Nicoletti, R. Elhage, M. Rudling, H.G. Ljunggren, G.K. Hansson, and G.P. Berne. 2004. CD1d-dependent activation of NKT cells aggravates atherosclerosis. *J. Exp. Med*. 199:417–422.
15. Paulsson, G., X. Zhou, E. Tornquist, and G.K. Hansson. 2000. Oligoclonal T cell expansions in atherosclerotic lesions of apolipoprotein E-deficient mice. *Arterioscler. Thromb. Vasc. Biol*. 20:10–17.

16. de Boer, O.J., A.E. Becker, and A.C. van der Wal. 2003. T lymphocytes in atherogenesis-functional aspects and antigenic repertoire. *Cardiovasc. Res.* 60:78–86.
17. Parums, D., and M.J. Mitchinson. 1981. Demonstration of immunoglobulin in the neighbourhood of advanced atherosclerotic plaques. *Atherosclerosis.* 38:211–216.
18. Zhou, X., and G.K. Hansson. 1999. Detection of B cells and proinflammatory cytokines in atherosclerotic plaques of hypercholesterolaemic apolipoprotein E knockout mice. *Scand. J. Immunol.* 50:25–30.
19. Binder, C.J., and G.J. Silverman. 2005. Natural antibodies and the autoimmunity of atherosclerosis. *Springer Semin. Immunopathol.* 26:385–404.
20. Wick, G., M. Romen, A. Amberger, B. Metzler, M. Mayr, G. Falkensammer, and Q. Xu. 1997. Atherosclerosis, autoimmunity, and vascular-associated lymphoid tissue. *FASEB J.* 11:1199–1207.
21. Angeli, V., J. Llodra, J.X. Rong, K. Satoh, S. Ishii, T. Shimizu, E.A. Fisher, and G.J. Randolph. 2004. Dyslipidemia associated with atherosclerotic disease systemically alters dendritic cell mobilization. *Immunity.* 21:561–574.
22. Faggiotto, A., R. Ross, and L. Harker. 1984. Studies of hypercholesterolemia in the nonhuman primate. I. Changes that lead to fatty streak formation. *Arteriosclerosis.* 4:323–340.
23. Gerrity, R.G., and H.K. Naito. 1980. Ultrastructural identification of monocyte-derived foam cells in fatty streak lesions. *Artery.* 8:208–214.
24. Osterud, B., and E. Bjorklid. 2003. Role of monocytes in atherogenesis. *Physiol. Rev.* 83:1069–1112.
25. Smith, J.D., E. Trogan, M. Ginsberg, C. Grigaux, J. Tian, and M. Miyata. 1995. Decreased atherosclerosis in mice deficient in both macrophage colony-stimulating factor (op) and apolipoprotein E. *Proc. Natl. Acad. Sci. USA.* 92:8264–8268.
26. Bonanno, E., A. Mauriello, A. Partenzi, L. Anemona, and L.G. Spagnoli. 2000. Flow cytometry analysis of atherosclerotic plaque cells from human carotids: a validation study. *Cytometry.* 39:158–165.
27. Liu-Wu, Y., A. Svenningsson, S. Stemme, J. Holm, and O. Wiklund. 1997. Identification and analysis of macrophage-derived foam cells from human atherosclerotic lesions by using a "mock" FL3 channel in flow cytometry. *Cytometry.* 29:155–164.
28. Tavian, M., L. Coulombel, D. Luton, H.S. Clemente, F. Dieterlen-Lievre, and B. Peault. 1996. Aorta-associated $CD34^+$ hematopoietic cells in the early human embryo. *Blood.* 87:67–72.
29. Mombaerts, P., J. Iacomini, R.S. Johnson, K. Herrup, S. Tonegawa, and V.E. Papaioannou. 1992. RAG-1-deficient mice have no mature B and T lymphocytes. *Cell.* 68:869–877.
30. Arbones, M.L., D.C. Ord, K. Ley, H. Ratech, C. Maynard-Curry, G. Otten, D.J. Capon, and T.F. Tedder. 1994. Lymphocyte homing and leukocyte rolling and migration are impaired in L-selectin-deficient mice. *Immunity.* 1:247–260.
31. Streeter, P.R., B.T. Rouse, and E.C. Butcher. 1988. Immunohistologic and functional characterization of a vascular addressin involved in lymphocyte homing into peripheral lymph nodes. *J. Cell Biol.* 107: 1853–1862.
32. Hogquist, K.A., S.C. Jameson, W.R. Heath, J.L. Howard, M.J. Bevan, and F.R. Carbone. 1994. T cell receptor antagonist peptides induce positive selection. *Cell.* 76:17–27.
33. Binder, C.J., K. Hartvigsen, M.K. Chang, M. Miller, D. Broide, W. Palinski, L.K. Curtiss, M. Corr, and J.L. Witztum. 2004. IL-5 links adaptive and natural immunity specific for epitopes of oxidized LDL and protects from atherosclerosis. *J. Clin. Invest.* 114:427–437.
34. Bjorkbacka, H., V.V. Kunjathoor, K.J. Moore, S. Koehn, C.M. Ordija, M.A. Lee, T. Means, K. Halmen, A.D. Luster, D.T. Golenbock, and M.W. Freeman. 2004. Reduced atherosclerosis in MyD88-null mice links elevated serum cholesterol levels to activation of innate immunity signaling pathways. *Nat. Med.* 10:416–421.
35. Hansson, G.K., P. Libby, U. Schonbeck, and Z.Q. Yan. 2002. Innate and adaptive immunity in the pathogenesis of atherosclerosis. *Circ. Res.* 91:281–291.
36. Butcher, E.C. 1991. Leukocyte-endothelial cell recognition: three (or more) steps to specificity and diversity. *Cell.* 67:1033–1036.
37. Eriksson, E.E., X. Xie, J. Werr, P. Thoren, and L. Lindbom. 2001. Direct viewing of atherosclerosis in vivo: plaque invasion by leukocytes is initiated by the endothelial selectins. *FASEB J.* 15:1149–1157.
38. Huo, Y., C. Weber, S.B. Forlow, M. Sperandio, J. Thatte, M. Mack, S. Jung, D.R. Littman, and K. Ley. 2001. The chemokine KC, but not monocyte chemoattractant protein-1, triggers monocyte arrest on early atherosclerotic endothelium. *J. Clin. Invest.* 108:1307–1314.
39. Eriksson, E.E., X. Xie, J. Werr, P. Thoren, and L. Lindbom. 2001. Importance of primary capture and L-selectin-dependent secondary capture in leukocyte accumulation in inflammation and atherosclerosis in vivo. *J. Exp. Med.* 194:205–218.
40. Stemme, S., J. Holm, and G.K. Hansson. 1992. T lymphocytes in human atherosclerotic plaques are memory cells expressing CD45RO and the integrin VLA-1. *Arterioscler. Thromb.* 12:206–211.
41. Baumgarth, N., O.C. Herman, G.C. Jager, L. Brown, L.A. Herzenberg, and L.A. Herzenberg. 1999. Innate and acquired humoral immunities to influenza virus are mediated by distinct arms of the immune system. *Proc. Natl. Acad. Sci. USA.* 96:2250–2255.
42. Horkko, S., D.A. Bird, E. Miller, H. Itabe, N. Leitinger, G. Subbanagounder, J.A. Berliner, P. Friedman, E.A. Dennis, L.K. Curtiss, et al. 1999. Monoclonal autoantibodies specific for oxidized phospholipids or oxidized phospholipid-protein adducts inhibit macrophage uptake of oxidized low-density lipoproteins. *J. Clin. Invest.* 103:117–128.
43. Bobryshev, Y.V., and R.S. Lord. 1995. Ultrastructural recognition of cells with dendritic cell morphology in human aortic intima. Contacting interactions of vascular dendritic cells in athero-resistant and atherosprone areas of the normal aorta. *Arch. Histol. Cytol.* 58:307–322.
44. Llodra, J., V. Angeli, J. Liu, E. Trogan, E.A. Fisher, and G.J. Randolph. 2004. Emigration of monocyte-derived cells from atherosclerotic lesions characterizes regressive, but not progressive, plaques. *Proc. Natl. Acad. Sci. USA.* 101:11779–11784.
45. Cupedo, T., W. Jansen, G. Kraal, and R.E. Mebius. 2004. Induction of secondary and tertiary lymphoid structures in the skin. *Immunity.* 21:655–667.
46. Moos, M.P., N. John, R. Grabner, S. Nossmann, B. Gunther, R. Vollandt, C.D. Funk, B. Kaiser, and A.J. Habenicht. 2005. The lamina adventitia is the major site of immune cell accumulation in standard chow-fed apolipoprotein E-deficient mice. *Arterioscler. Thromb. Vasc. Biol.* 25:2386–2391.
47. Zhang, S.H., R.L. Reddick, J.A. Piedrahita, and N. Maeda. 1992. Spontaneous hypercholesterolemia and arterial lesions in mice lacking apolipoprotein E. *Science.* 258:468–471.
48. Mullins, D.W., T.N. Bullock, T.A. Colella, V.V. Robila, and V.H. Engelhard. 2001. Immune responses to the HLA-A*0201-restricted epitopes of tyrosinase and glycoprotein 100 enable control of melanoma outgrowth in HLA-A*0201-transgenic mice. *J. Immunol.* 167: 4853–4860.